Hindawi
Journal of Applied Mathematics
Volume 2023, Article ID 2549560, 11 pages
https://doi.org/10.1155/2023/2549560

Research Article

Analytic Solutions of 2D Cubic Quintic Complex Ginzburg-Landau Equation

F. Waffo Tchuimmo,[1] J. B. Gonpe Tafo,[1,2] A. Chamgoue,[3] N. C. Tsague Mezamo,[1] F. Kenmogne,[4] and L. Nana[1]

[1]*Department of Physics, Faculty of Science, Pure Physics, Laboratory, Group of Nonlinear Physics and Complex Systems, University of Douala, P.O. Box 24157, Douala, Cameroon*
[2]*Department of Base Scientific Education, Advanced Teacher's Training College of the Technical Education, University of Douala, P.O. Box 8213, Douala, Cameroon*
[3]*Department of Physics, School of Geology and Mining Engineering, University of Ngaoundéré, P.O. Box 115 Meiganga, Cameroon*
[4]*Department of Civil Engineering, Advanced Teacher's Training College of the Technical Education, University of Douala, P.O. Box 8213, Douala, Cameroon*

Correspondence should be addressed to J. B. Gonpe Tafo; joelgbruno@yahoo.fr

Received 8 November 2022; Revised 17 October 2023; Accepted 27 November 2023; Published 19 December 2023

Academic Editor: Oluwole D. Makinde

The dynamical behaviour of traveling waves in a class of two-dimensional system whose amplitude obeys the two-dimensional complex cubic-quintic Ginzburg-Landau equation is deeply studied as a function of parameters near a subcritical bifurcation. Then, the bifurcation method is used to predict the nature of solutions of the considered wave equation. It is applied to reduce the two-dimensional complex cubic-quintic Ginzburg-Landau equation to the quintic nonlinear ordinary differential equation, easily solvable. Under some constraints of parameters, equilibrium points are obtained and phase portraits have been plotted. The particularity of these phase portraits obtained for new ordinary differential equation is the existence of homoclinic or heteroclinic orbits depending on the nature of equilibrium points. For some parameters, one has the orbits starting to one fixed point and passing through another fixed point before returning to the same fixed point, predicting then the existence of the combination of a pair of pulse-dark soliton. One has also for other parameters, the orbits linking three equilibrium points predicting the existence of a dark soliton pair. These results are very important and can predict the same solutions in many domains, particularly in wave phenomena, mechanical systems, or laterally heated fluid layers. Moreover, depending on the values of parameter systems, the analytical expression of the solutions predicted is found. The three-dimensional graphs of these solutions are plotted as well as their 2D plots in the propagation direction.

1. Introduction

During the past three decades, considerable progresses have been made in the spontaneous emergence of patterns in spatially extended nonequilibrium systems. The existence of spatiotemporal patterns has been deeply established on the basis of equivariant bifurcation theory [1, 2]. Patterns resulting from a symmetry-breaking Hopf bifurcation are especially vulnerable to instability. Particularly, the extended nonlinear dynamical systems display an amazing variety of behaviours, namely, pattern formation, self-organization, and spatiotemporal chaos [3, 4].

Much effort has been devoted to the modeling of different dynamical regimes and the transitions between them by nonlinear partial differential equations (NPDEs). NPDEs play considerable roles in several scientific and engineering fields. Among the NPDEs, one can cite the Korteweg-de Vries equation, the van der Waals equation, the nonlinear Schrödinger equation, the Navier-Stokes equation, the magnetohydrodynamic equation, the Ginzburg-Landau equa-

tion, [5–10] and so on, all of them being used to describe the propagation of the wave in different matters. They have been extensively used in different branches of physics and applied mathematics. The Ginzburg-Landau equation is one of the models of NPDEs that has had notable success in characterizing evolution phenomena in a wide range of dynamical systems. In recent works of Gonpe et al. and Tafo et al. [11, 12], the one-dimensional complex cubic-quintic Ginzburg-Landau equation (CQGLE) was used to find many types of dynamical regimes, namely, the phase turbulence, weak turbulence, defect turbulence, spatiotemporal intermittency regimes, or laminar state. In order to understand the different nonlinear phenomena, many powerful methods to build exact solutions of nonlinear evolution equations have been established and developed such as specially envelope transform and direct ansatz method, successfully used to obtain a type of chirped bright and dark solitary waves as solutions of one-dimensional cubic Ginzburg-Landau equation [13, 14]; the one-soliton and two-soliton solutions of the derivative NLS equations were found by using the Hirota bilinear method as well as the square operator method [15–17], the exponential function approach [18], the similarity transformation [19, 20], and the network method [21]. The periodic and blow-up solutions for two-dimensional Ginzburg-Landau equation were obtained by using the homogeneous balance principle, the general Jacobi elliptic function method [22], the Riccati-Bernoulli sub-ODE method [23, 24] the sine-cosine approach [25, 26], and the Cole-Hopf transformation method [27] which are applied for the constructing of many new exact solutions, as well as the bifurcation theory for planar dynamical systems to the two-dimensional cubic complex Ginzburg-Landau equation [28] and so on.

In real physical systems, most one-dimensional studies are simplified versions of two or more dimensional ones. Many studies in 1D CQGLE have been done, and they show interesting results. However, the case of 2D CQGLE is more complex, and the studies of solutions obtained from this equation could give us new kinds of solutions, which can help in many domains. The author [28] worked in 2D GLE but in the cubic case by using the bifurcation theory. He found three equilibrium points and established analytical solutions around equilibrium points. This is why the research field in this light is steel-opened and deserves particular attention. The present work is aimed at extending the study in the case of 2D CQGLE in an anisotropic system by using bifurcation theory for a planar dynamical system in order to construct new traveling wave solutions. Let us now consider the 2D CQGLE as given in [28–30]

$$iA_t + \frac{1}{2}A_{xx} + \frac{1}{2}(\alpha + ic_2)A_{yy} + (1 - ic_3)|A|^2A - (1 - ic_5)|A|^4A = i\sigma A, \tag{1}$$

where $A = A(x, y, t)$ is a complex wave amplitude, with $i^2 = -1$. (x, y) are the propagation coordinates and t is the retarded time, while α, c_2, c_3, c_5, and σ are real constants. The term proportional to α represents the linear dispersion, and c_2 is the diffusion coefficient in y direction. The terms proportional to parameters c_3 and c_5 represent the nonlinear dispersion of wave patterns, respectively. The term proportional to σ denotes the linear growth or damping. A weakly nonlinear and dissipative system having a canonical model can be expressed with the CQGLE. In order to justify the main motivation of the present work, let us outline that in [28], an equation in the form of Eq. (1) appears without the quintic terms proportional to $|A|^4A$, while the phase portraits plotted showing at maximum 3 equilibrium points were obtained and used to predict the nature of solutions and then, some exact traveling wave solutions were constructed. In [29], Eq. (1) was found, but the coefficient of the quintic term is proportional to $i\gamma$, then its real part was zero, and the plot of solutions was obtained numerically by means of a pseudospectral algorithm, taking arbitrary the Gaussian form as an initial waveform as $u = 2\exp[-1/4(x^2 + y^2)]$, which is a hard problem. The equation found in [30] is identical to that found in [29], and some localized explicit solutions were computed, although they were not predicted via the bifurcation of phase portraits. In the recent works of Shtyrina et al. [31], some solutions of the CQGLE were found, but in the implicit forms. These works concerning the Ginzburg-Landau equation and particularly the 2D cases justify that the field of studies on these equations is still open and deserves particular attention. This is why in the present work, we carry an emphasis on the bifurcation of phase portraits in order to predict the nature of solutions of the CQGLE, and moreover, we seek additional solutions as those periodic, which to the best of our knowledge were not been done before.

The outline of this paper is as follows: In Section 2.1, we convert the 2D CQGLE into a traveling wave system that is proved to be the Hamiltonian system, followed by the finding of equilibrium points and the study of bifurcation of phase portraits for the traveling wave system. In Section 3.1, we find some exact solutions. In Section 3.4, the graphical representation of some solutions is provided. Next, in Section 4, we study the stability of modulated wave in the system, and finally, in Section 5, a conclusion and perspective are made.

2. Equilibrium Points and Bifurcation of Phase Portraits

2.1. Preliminary. In this section, we transform the 2D CQGLE into a nonlinear ordinary differential equation, easily solvable. To do this, let us assume the traveling solution of Eq. (1) in the form [28, 32–34]

$$A(x, y, t) = \exp(i\eta)\varphi(x, y, t), \eta = px + st, \tag{2}$$

where $\varphi(x, y, t)$ is a real function, while p and s are the wave number and spectral parameter, respectively. Inserting Eq. (2) into Eq. (1), one obtains

$$\begin{aligned} i(\varphi_t + is\varphi) + \frac{1}{2}\left(\varphi_{xx} + 2ip\varphi_x - p^2\varphi\right) + \frac{1}{2}(\alpha + ic_2)\varphi_{yy} \\ + (1 - ic_3)\varphi^3 - (1 - ic_5)\varphi^5 = i\sigma\varphi, \end{aligned} \tag{3}$$

which can be separated into the real and imaginary parts to give

$$\begin{cases} \varphi_t - \frac{1}{2}c_2\varphi_{yy} - \sigma\varphi + p\varphi_x - c_3\varphi^3 + c_5\varphi^5 = 0, \\ \frac{1}{2}\left(\varphi_{xx} + \alpha\varphi_{yy}\right) - \left(s + \frac{1}{2}p^2\right)\varphi + \varphi^3 - \varphi^5 = 0. \end{cases} \tag{4}$$

Let us assume that

$$\varphi(x, y, t) = \Psi(\xi) \text{ with } \xi = fx + gy + ht, \tag{5}$$

where f and g are connected as $f^2 + g^2 = 1$ and h is an arbitrary constant. Substituting Eq. (5) into Eq. (4), we get after many transformations the nonlinear ODE:

$$\ddot{\Psi} - a_1\Psi + a_3\Psi^3 - a_5\Psi^5 = 0, \tag{6}$$

with

$$\begin{aligned} a_1 &= \frac{2s + c_1p^2}{f^2 + \alpha g^2}, \\ a_3 &= \frac{2}{f^2 + \alpha g^2}, \\ a_5 &= \frac{2}{f^2 + \alpha g^2}. \end{aligned} \tag{7}$$

Let $d\Psi/d\xi = z$, then Eq. (6) is equivalent to the following planar dynamical system:

$$\begin{cases} \dot{\Psi} = z, \\ \dot{z} = a_1\Psi - a_3\Psi^3 + a_5\Psi^5. \end{cases} \tag{8}$$

Equation (6) can be integrated upon multiplication by $\dot{\Psi}$ to give the following Hamiltonian:

$$H = \frac{1}{2}\dot{\Psi}^2 - \frac{a_1}{2}\Psi^2 + \frac{a_3}{4}\Psi^4 - \frac{a_5}{6}\Psi^6, \tag{9}$$

which is a conserved quantity for the system (Eq. (8)).

2.2. Equilibrium Points. In this section, we seek the equilibrium points and plot some phase portraits for a range of the system parameters. These equilibrium points are obtained by setting in the system (Eq. (8)) the constraints $(\dot{\Psi}, \dot{z}) = (0, 0)$. Therefore, they can be written as $(\Psi_0, z_0 = 0)$, where Ψ_0 is the zeros of the following polynomial function:

$$a_1\Psi - a_3\Psi^3 + a_5\Psi^5 = 0, \tag{10}$$

leading to the following set of solutions:

$$\xi_0 = (0, 0), \xi_{1,2,3,4} = \left(\pm\sqrt{\frac{a_3 \pm \sqrt{a_3^2 - 4a_1a_5}}{2a_5}}, 0\right), \tag{11}$$

2.3. Bifurcation of Phase Portraits. Some cases can be observed as follows:

(i) Case 1 ($a_3^2 - 4a_1a_5 < 0$). Whatever the value of a_3, the system has a single equilibrium point $(0, 0)$, which can be a saddle point when $a_1 < 0$ and $a_5 < 0$ or a stable equilibrium point when $a_1 > 0$ and $a_5 > 0$

(ii) Case 2 ($a_3^2 - 4a_1a_5 > 0$). In this case, three equilibrium points are observed, and one can distinguish two types of situations

The first one, which is obtained for $a_1 > 0$, $a_3 > 0$, and $a_5 < 0$, and one has two symmetric equilibrium points Ψ_1 and Ψ_2 given by $\Psi_{1,2} = (\pm\sqrt{a_3 - \sqrt{a_3^2 - 4a_1a_5}/2a_5}, 0)$, which are saddle points, and fixed point $\Psi_0 = (0, 0)$ which is a center. In this case, the separatrix connects Ψ_1 to Ψ_2 and is qualified as a heteroclinic orbit because two distinct unstable equilibrium points are concerned. In fact, the heteroclinic orbit (sometimes called a heteroclinic connection) is a path in phase space which joins two different equilibrium points. This separatrix separates bounded, periodic oscillatory motions around Ψ_0 from unbounded nonperiodic ones.

The second one is obtained for, $a_1 < 0$, $a_3 < 0$, and $a_5 > 0$, and the system has also 3 equilibrium points which are as follows: the origin $\Psi_0 = (0, 0)$ which is the saddle points, and $\Psi_{1,2} = (\pm\sqrt{a_3 + \sqrt{a_3^2 - 4a_1a_5}/2a_5}, 0)$ which are the center points. The separatrix here connects the point Ψ_0 to itself. It is qualified as a homoclinic orbit because a single unstable equilibrium point is involved in the connection. A homoclinic orbit is a trajectory of a flow of a dynamical system which joins a saddle equilibrium point to itself. This separatrix is the boundary between confined-in-wells periodic motions and cross-wells periodic motions. It is obvious that the plots of the two cases above are not new and were already been sketched in [28] in the context of cubic case.

(iii) Case 3. As plotted in Figures 1(a) and 1(c), obtained for $a_3^2 - 4a_1a_5 > 0$, $a_1 > 0$, $a_3 > 0$, and $a_5 > 0$. In this case, the system has 5 equilibrium points which are $\Psi_0 = (0, 0)$, corresponding to a center point, $\Psi_{1,2} = (\pm\sqrt{a_3 + \sqrt{a_3^2 - 4a_1a_5}/2a_5}, 0)$ and $\Psi_{3,4} = (\pm\sqrt{a_3 - \sqrt{a_3^2 - 4a_1a_5}/2a_5}, 0)$. As one can see, $\Psi_{1,2}$ are stable, while the others, Ψ_0 and $\Psi_{3,4}$, are saddle points. The particularity of the potential here is that all the unstable fixed points are on the same potential level (the same holds for the stable ones). For this case, there are two pairs of heteroclinic orbits. The profile of the potential and the phase portrait are depicted in Figure 1(c)

(iv) Case 4, which corresponds to the Figures 1(b) and 1(d). In this last case, one has $a_3^2 - 4a_1a_5 > 0$, $a_1 < 0$, and $a_5 < 0$, and the system has 5 equilibrium points. The stable fixed points $\Psi_0 = (0, 0)$ and $\Psi_{3,4} = (\pm\sqrt{a_3 - \sqrt{a_3^2 - 4a_1a_5}/2a_5}, 0)$, and unstable ones $\Psi_{1,2} = (\pm\sqrt{a_3 + \sqrt{a_3^2 - 4a_1a_5}/2a_5}, 0)$. In this

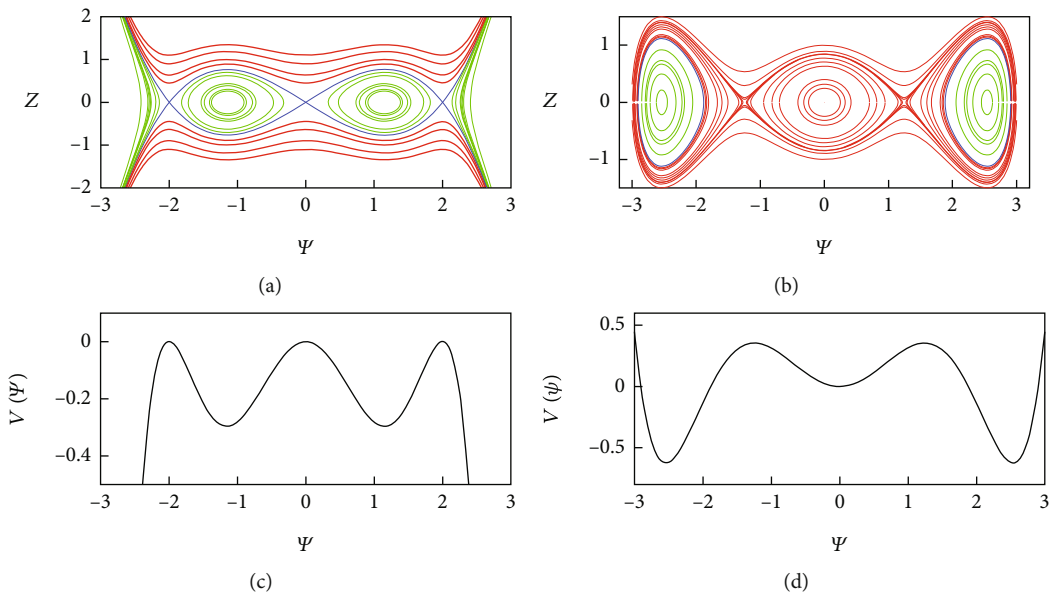

FIGURE 1: Phase portrait for different values of h in (a) and (b) for five equilibrium points, and corresponding potentials in (c) and (d). In (a), one has the heteroclinic orbit, which is the curve starting at one fixed point and ending at another fixed point predicting the existence of kink or dark soliton as solution. In (b), one has the separatrix which appears as the combination of homoclinic and heteroclinic orbits, predicting then the existence of a bright-dark soliton pair as solution. This last case, due to the presence of the quintic term, cannot be obtained in the cubic case as in [28].

configuration, homoclinic orbits as well as heteroclinic exist simultaneously

3. The Analytical Solutions of the 2D CQGLE

3.1. Preliminary. The exact solutions of the 2D CQGLE (1) are found by using the Jacobi elliptic properties. Thus, by using the energy integral Eq. (9), separating the variables, and integrating both sides, one obtains

$$\int_{\xi_0}^{\xi} d\xi = \int_0^{\Psi} \frac{d\psi}{\sqrt{2h - a_1\psi^2 + (a_3/2)\psi^4 - (a_5/3)\psi^6}}, \tag{12}$$

which can be rewritten in the form as follows:

$$\int_{\xi_0}^{\xi} d\xi = \int_0^{\Psi} \frac{d\psi}{\sqrt{-a_5/3(-(6h/a_5) + (3a_1/a_5)\psi^2 - (3a_3/2a_5)\psi^4 + \psi^6)}}, \tag{13}$$

Let us factorize the high degree polynomial in integral expression (Eq. (13)), leading to the following:

$$\int_{\xi_0}^{\xi} d\xi = \int_0^{\Psi} \frac{d\psi}{\sqrt{-a_5/3\left(\psi^2 - \psi_1^2\right)\left(\psi^2 - \psi_2^2\right)\left(\psi^2 - \psi_3^2\right)}}, \tag{14}$$

where ψ_1 is a real number and ψ_2 and ψ_3 are the complex conjugations. The solutions are obtained using the Cardan method as follows:

$$\begin{aligned}
&\psi_1 = U + V,\\
&\psi_2 = jU + jV\ \psi_3 = jU + jV,\\
&j = \exp\left(i\frac{2\pi}{3}\right),\\
&U = \sqrt{\frac{-Q + \sqrt{\Delta}}{2}},\\
&V = \sqrt{\frac{-Q - \sqrt{\Delta}}{2}},\\
&\Delta = Q^2 + \frac{4}{27}P^3,\\
&Q = -\frac{a_3}{2a_5}\left(\frac{a_3^2}{2a_5^2} - \frac{3a_1}{a_5}\right) - \frac{6H}{a_5},\\
&P = -\frac{3a_3^2}{a_5^2} + \frac{3a_1}{a_5}.
\end{aligned} \tag{15}$$

Then, one can obtain many kinds of solutions of Eq. (14) depending on the special choices for a_5 [35–37].

3.2. Case (a) $a_5 < 0$. For this case, the exact solution of the traveling waves is obtained by integrating Eq. (14) as follows:

$$\int_{\xi_0}^{\xi} d\xi = \int_0^{\Psi} \frac{d\psi}{\sqrt{-a_5/3\left(\psi^2 - \psi_1^2\right)\left(\psi^2 - \psi_2^2\right)\left(\psi^2 - \psi_3^2\right)}}. \tag{16}$$

The solution of this integral is obtained using the integration tables as given in [35] (see pages 259 and 260 of the reference).

$$\Psi(\xi) = \frac{\psi_1}{\sqrt{1 - B_1/C_1(1 + \mathrm{cn}(2\mu_1(\xi - \xi_0), K_1))/(1 - \mathrm{cn}(2\mu_1(\xi - \xi_0), K_1))}}, \tag{17}$$

$$\begin{aligned} C_1 &= \psi_2\psi_3, \\ B_1^2 &= \left(\psi_1^2 - \psi_2^2\right)\left(\psi_1^2 - \psi_3^2\right), \\ K_1^2 &= \frac{(C_1 + B_1)^2 - \psi_1^4}{4B_1C_1}, \\ \mu_1 &= \sqrt{-\nu}, \\ \nu &= \frac{a_5}{3}B_1C_1. \end{aligned} \tag{18}$$

After using the following properties of Jacobi elliptic functions,

$$\begin{aligned} \frac{1 + \mathrm{cn}(2\mu_1(\xi - \xi_0), K_1)}{1 - \mathrm{cn}(2\mu_1(\xi - \xi_0), K_1)} &= \frac{\mathrm{cn}^2(\mu_1(\xi - \xi_0), K_1)}{\mathrm{sn}^2(\mu_1(\xi - \xi_0), K_1)\mathrm{dn}^2(\mu_1(\xi - \xi_0), K_1)}, \\ \mathrm{sn}(\mu_1(\xi - \xi_0) + K_1, K_1) &= \frac{\mathrm{cn}(\mu_1(\xi - \xi_0), K_1)}{\mathrm{dn}(\mu_1(\xi - \xi_0), K_1)} \end{aligned} \tag{19}$$

one obtains the final expression

$$\Psi(\xi) = \frac{\psi_1}{\sqrt{1 - B_1(\mathrm{sn}^2(\mu_1(\xi - \xi_0) + K_1, K_1))/C_1(\mathrm{sn}^2(\mu_1(\xi - \xi_0), K_1))}}. \tag{20}$$

The exact traveling wave solution for Eq. (1) has the form

$$A(x, y, t) = \frac{\psi_1}{\sqrt{1 - B_1(\mathrm{sn}^2(\mu_1(f(x - x_0) + g(y - y_0) + ht) + K_1, K_1))/C_1(\mathrm{sn}^2(\mu_1(f(x - x_0) + g(y - y_0) + ht), K_1))}} \exp\left(i(px + st)\right). \tag{21}$$

3.2.1. Special Cases

(i) When $K_1 = 0$, in this case, the expression of Eq. (20) can be rewritten in the form

$$\Psi(\xi) = \frac{\psi_1}{\sqrt{1 + \gamma_1 \cot^2(\mu_3(\xi - \xi_0))}}, \tag{22}$$

leading to

$$A(x, y, t) = \frac{\psi_1}{\sqrt{1 + \gamma_1 \cot^2(\mu_3(f(x - x_0) + g(y - y_0) + ht))}} \exp\left(i(px + st)\right), \tag{23}$$

where $\mu_3 = \sqrt{-\nu_1}$, and

$$\begin{aligned} \gamma_1 &= 1 - \frac{\psi_1^2}{\psi_2\psi_3}, \\ \nu_1 &= \frac{a_5}{3}\left(\psi_1^2 - \psi_2\psi_3\right)\psi_2\psi_3. \end{aligned} \tag{24}$$

(ii) When $K_1 = 1$, in this case, the expression of Eq. (22) becomes

$$\Psi(\xi) = \frac{\psi_1}{\sqrt{1 - \gamma_1 \coth^2(\mu_3(\xi - \xi_0))}}, \tag{25}$$

which leads to

$$A(x, y, t) = \frac{\psi_1}{\sqrt{1 - \gamma_1 \coth^2(\mu_3(f(x - x_0) + g(y - y_0) + ht))}} \exp\left(i(px + st)\right), \tag{26}$$

3.3. Case (a) $a_5 > 0$. In this, one can simplify Eq. (14) in the form

$$\int_{\xi_0}^{\xi} d\xi = \int_0^{\Psi} \frac{d\psi}{\sqrt{(a_5/3)\left(\psi_1^2 - \psi^2\right)\left(\psi^2 - \psi_2^2\right)\left(\psi^2 - \psi_3^2\right)}}. \tag{27}$$

After using the same integration tables and the simplification tables of the elliptic function as done up, one can obtain

$$\Psi(\xi) = \psi_1 \frac{1}{\sqrt{1 + B_1(\mathrm{sn}^2(\mu_2(\xi - \xi_0) + K_2, K_2))/C_1(\mathrm{sn}^2(\mu_2(\xi - \xi_0), K_2))}}, \tag{28}$$

$$(x, y, t) = \psi_1 \frac{1}{\sqrt{1 + B_1(\mathrm{sn}^2(\mu_2(f(x - x_0) + g(y - y_0) + ht) + K_2, K_2))/C_1(\mathrm{sn}^2(\mu_2(f(x - x_0) + g(y - y_0) + ht), K_2))}} \exp\left(i(px + st)\right), \tag{29}$$

where $K_2^2 = -K_1^2$ and $\mu_2 = \sqrt{\nu}$. K_1, ν, B_1, and C_1 are being defined in Eq. (18).

3.3.1. Special Cases

(i) When $K_2 = 0$, in this case, the expression of Eq. (28) can be rewritten in the form

$$\Psi(\xi) = \frac{\psi_1}{\sqrt{1 - \gamma_1^{-1} \cot^2(\mu_4(\xi - \xi_0))}}, \tag{30}$$

leading to

$$A(x, y, t) = \frac{\psi_1}{\sqrt{1 - \gamma_1^{-1} \cot^2(\mu_4(f(x - x_0) + g(y - y_0) + ht))}} \times \exp\,(i(px + st)), \tag{31}$$

where $\mu_4 = \sqrt{-\nu_1}$.

(ii) When $K_2 = 1$, the expression of Eq. (28) reduces to

$$\Psi(\xi) = \frac{\psi_1}{\sqrt{1 + \gamma_1^{-1} \coth^2(\mu_6(\xi - \xi_0))}}, \tag{32}$$

leading to

$$A(x, y, t) = \frac{\psi_1}{\sqrt{1 + \gamma_1^{-1} \coth^2(\mu_4(f(x - x_0) + g(y - y_0) + ht))}} \times \exp\,(i(px + st)), \tag{33}$$

3.4. The Result: Some Graphs of Solutions. Here, some 2D and 3D shape graphics are illustrated for some selected solutions, for particular values of parameters. Figure 2 is related to the case where $a_5 < 0$ obtained by plotting solution (Eq. (21)), which appears as a train of the combination of pulse-dark soliton pair. However, Figure 3 is obtained for the case $a_5 > 0$ by plotting solution (29), which shows the train of solution.

The pictures relating to Eqs. (26) and (33) are observed in Figures 4 and 5. Figure 4 is the dark soliton called also "hole solution" [38]. The holes are characterized by a local concentration of the phase gradient and a depression of the wave amplitude $|A|$. The one-parameter family of traveling hole solutions discovered by Gradshteyn and Ryzhik [39] has been proved to play an important role in a large portion of nonlinear dynamical space systems, including in a region where they are linearly unstable. Figure 5 represents the bright-dark soliton pair, which was predicted by the appearance of the combination of homoclinic and heteroclinic orbits obtained in Figure 1(b) [40]. This is why Figures 2 and 3 can be viewed here as the train of bright-dark soliton, since Eqs. (26) and (33) are obtained for particular constraints on the parameters of Eqs. (21) and (29). The same type of profile was found in [33, 41], although both solutions are different. Then, the solutions with profile described by Eqs. (26) and (33) can describe some complex phenomena observed in applied sciences and engineering, like fluid dynamics, quantum physics, particles, and nuclear physics.

4. Stability Analysis

In this section, we study the stability conditions of the modulated waves governed by some solutions found in Section 3.1. To this end, let us remember that several methods have been used to investigate the stability of modulated waves among which the perturbation method, known as modulational instability (MI) [42] as well as the Vakhitov-Kolokolov stability criterion for a single pulse soliton [43, 44].

4.1. Stability Analysis: The Vakhitov-Kolokolov Stability Criterion. Remembering the so-called Vakhitov-Kolokolov stability criterion, the single pulse solution of the nonlinear Schrödinger equation and its extension is stable if its norm defined as

$$N = \int_{-\infty}^{+\infty} \left(\Psi(\xi)^2\right) d\xi \tag{34}$$

is an increasing function of the speed or the spectral parameter $(-s)$ as defined in Eq. (2). For the kink or dark soliton, it has been proved that the stability is connected to the renormalized norm defined as [44]

$$\tilde{N} = \int_{-\infty}^{+\infty} \left(\Psi_{\max}^2 - \Psi(\xi)^2\right) d\xi. \tag{35}$$

Dark soliton is stable whether $\tilde{N}$ is an increasing function of the speed or spectral parameter $(-s)$. For the dark soliton defined in Eq. (26) and plotted in Figure 4, the maximum found is $\Psi_{\max} = \psi_1/\sqrt{1 - \gamma_1}$, leading to the following expression of the renormalyzed norm

$$\tilde{N} = \frac{6}{a_5\sqrt{(\psi_1^2 - \psi_2\psi_3)\psi_2\psi_3}} = \frac{3(f^2 + \alpha g^2)}{\sqrt{(\psi_1^2 - \psi_2\psi_3)\psi_2\psi_3}}. \tag{36}$$

Eliminating f and g in the above equation by remembering Eq. (15) and that $f^2 + g^2 = 1$, one has

$$\tilde{N} = \frac{-3s + 3(\Psi_1^2 - C_1 p^2)/2 - \Psi_1^4}{h\sqrt{(\psi_1^2 - \psi_2\psi_3)\psi_2\psi_3}}, \tag{37}$$

from where it is obvious that dark soliton defined by Eq. (26) is an increasing function of $(-s)$, with the constraint $(\psi_1^2 - \psi_2\psi_3)\psi_2\psi_3 > 0$ and consequently is stable. For periodic solutions, the method outlined in this subsection is not adequate, and the stability will be found by the investigation of the MI criteria.

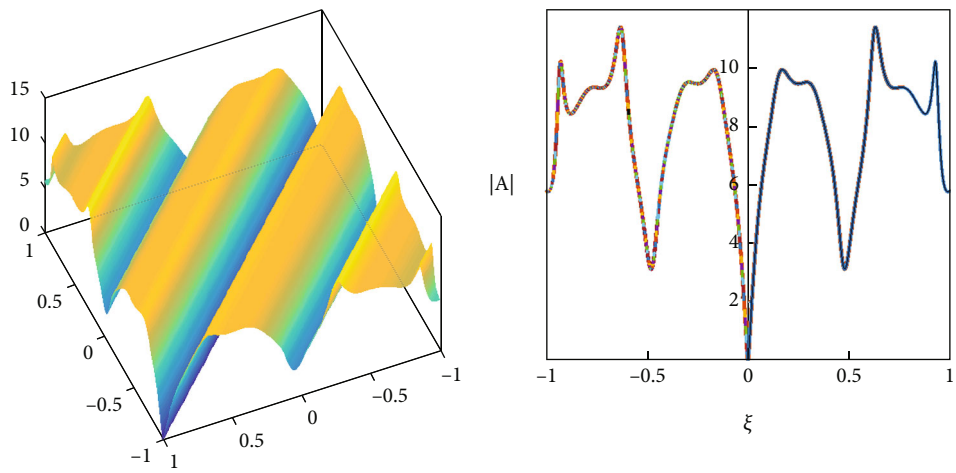

(a) (b)

Figure 2: Profile of periodic solution given by Eq. (21). (a) 3D plot. (b) Projection in the ξ direction for the parameters $a_1 = 0.5$, $a_3 = 1.0$, and $a_5 = -0.05$.

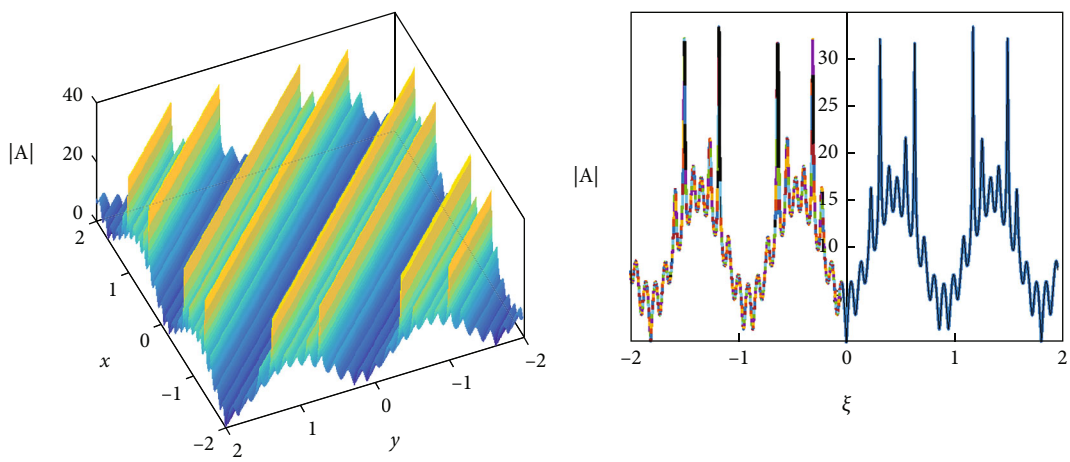

(a) (b)

Figure 3: Profile of solution given by Eq. (34). (a) 3D plot. (b) Projection in the ξ direction for the parameters $a_1 = 1.0$, $a_3 = 1.0$, and $a_5 = 0.15$. As one can see, one has a profile nearly similar to the train of bright-dark soliton.

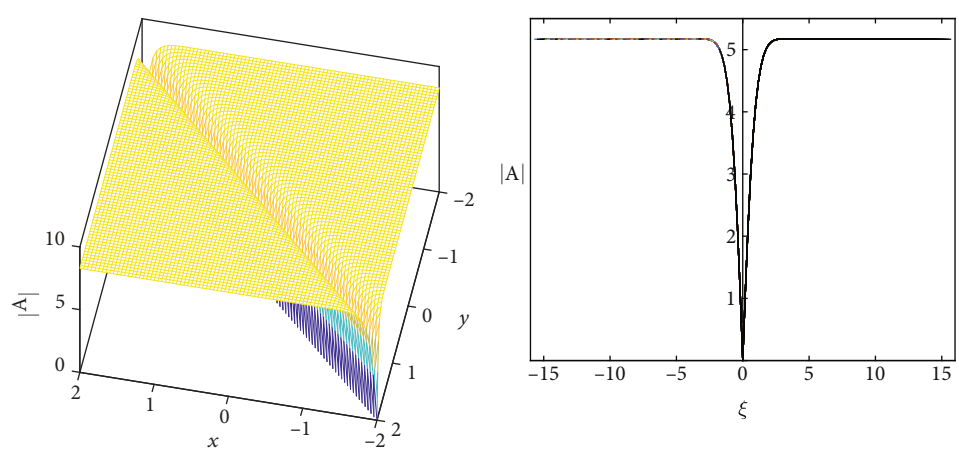

(a) (b)

Figure 4: Profile of solution given by Eq. (26). (a) 3D plot. (b) Projection in the ξ direction for the parameters $a_1 = -1.0$, $a_3 = 0.8$, and $a_5 = 0.1$. It corresponds to dark soliton predicted by the presence of heteroclinic orbits as plotted in Figure 1(b).

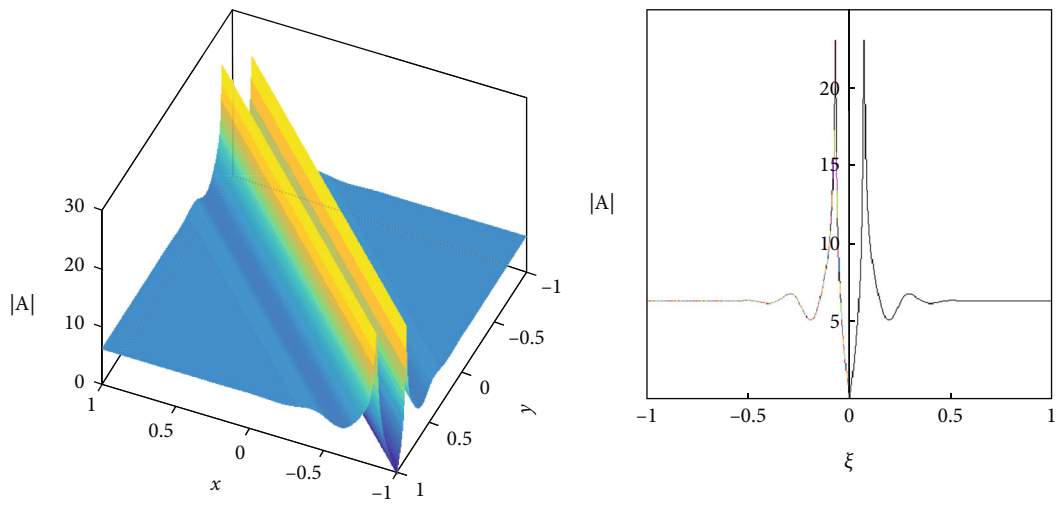

Figure 5: Profile of solution given by Eq. (33). (a) 3D plot. (b) Projection in the ξ direction for the parameters $a_1 = 1.0$, $a_3 = -2.0$, and $a_5 = -3/16$, showing the bright-dark soliton, corresponding to the combination of homoclinic and heteroclinic orbit.

4.2. Modulational Instability. In this subsection, we study the conditions under which the propagation of modulated waves in the network would become unstable to small perturbation; to this end, it is important to mention that Eq. (1) admits a solution in the form

$$\begin{aligned} A(x,y,t) &= A_0 \exp\left(i(g_0 - k_0 y)\right), \\ g_0 &= A_0^2 - A_0^4 + \left(\sigma + A0^2 c_3 - A_0^4 c_5\right)\frac{\alpha}{c_2}, \\ k_0 &= \sqrt{\frac{2\left(-\sigma + A_0^2\left(-c_3 + A_0^2 c_5\right)\right)}{c2}}. \end{aligned} \tag{38}$$

Let us now find the perturbed solution in the form [34, 41, 42]

$$A(x,y,t) = \left(A_0 + \varepsilon u(x,y,t)\right)\exp\left(i(g_0 - k_0 y)\right), \tag{39}$$

leading by inserting it into Eq. (1) and neglecting nonlinear terms to the following partial differential equation:

$$\begin{aligned} iu_t + \frac{1}{2}u_{xx} + \frac{1}{2}(\alpha + ic_2)u_{yy} + k_0(c_2 - i\alpha)u_y \\ + \left(1 - 2A_0^2 + i\left(2A_0^2 c_5 - c_3\right)\right)A_0^2(u+u)0. \end{aligned} \tag{40}$$

By taking the two-dimensional Fourier transform as $(k_x, k_y, t) = (1/2\pi)\int_{-\infty}^{\infty}\int_{-\infty}^{\infty} u(x,y,t)\exp\left(i(k_x x + k_y y)\right)dxdy$, Eq. (40) leads to

$$\begin{aligned} iU_t - \left(\frac{1}{2}k_x^2 + (\alpha + ic_2)\left(\frac{1}{2}k_y^2 - k_y k_0\right)\right)U \\ + \left(1 - 2A_0^2 + i\left(2A_0^2 c_5 - c_3\right)\right)A_0^2(U+U) = 0. \end{aligned} \tag{41}$$

Let us now express $U = U_1 + iU_2$, leading by separating Eq. (41) into real and imaginary parts to

$$\begin{cases} U_{1t} - \frac{1}{2}\left(k_x^2 + \alpha k_y\left(k_y - 2k_0\right)\right)U_2 + \left[-\frac{c_2}{2}k_y\left(k_y - 2k_0\right) + 2\left(2A_0^2 c_5 - c_3\right)A_0^2\right]U_1 = 0, \\ -U_{2t} + \left[-\frac{1}{2}\left(k_x^2 + \alpha k_y\left(k_y - 2k_0\right)\right) + 2\left(1 - 2A_0^2\right)A_0^2\right]U_1 + \frac{c_2}{2}k_y\left(k_y - 2k_0\right)U_2 = 0. \end{cases} \tag{42}$$

Let us find $U_1 = u_{01}\exp(-\gamma t)$, $U_2 = u_{02}\exp(-\gamma t)$, which can lead Eq. (42) to

$$\begin{pmatrix} \gamma + \frac{1}{2}c_2 k_y\left(2k_0 - k_y\right) + 2\left(2A_0^2 c_5 - c_3\right)A_0^2 - \frac{1}{2}\left(k_x^2 + \alpha k_y\left(k_y - 2k_0\right)\right) \\ 2\left(1 - 2A_0^2\right)A_0^2 - \frac{1}{2}\left(k_x^2 + \alpha k_y\left(k_y - 2k_0\right)\right) - \gamma - \frac{1}{2}c_2 k_y\left(2k_0 - k_y\right) \end{pmatrix}\begin{pmatrix} u_{01} \\ u_{02} \end{pmatrix} = \begin{pmatrix} 0 \\ 0 \end{pmatrix}. \tag{43}$$

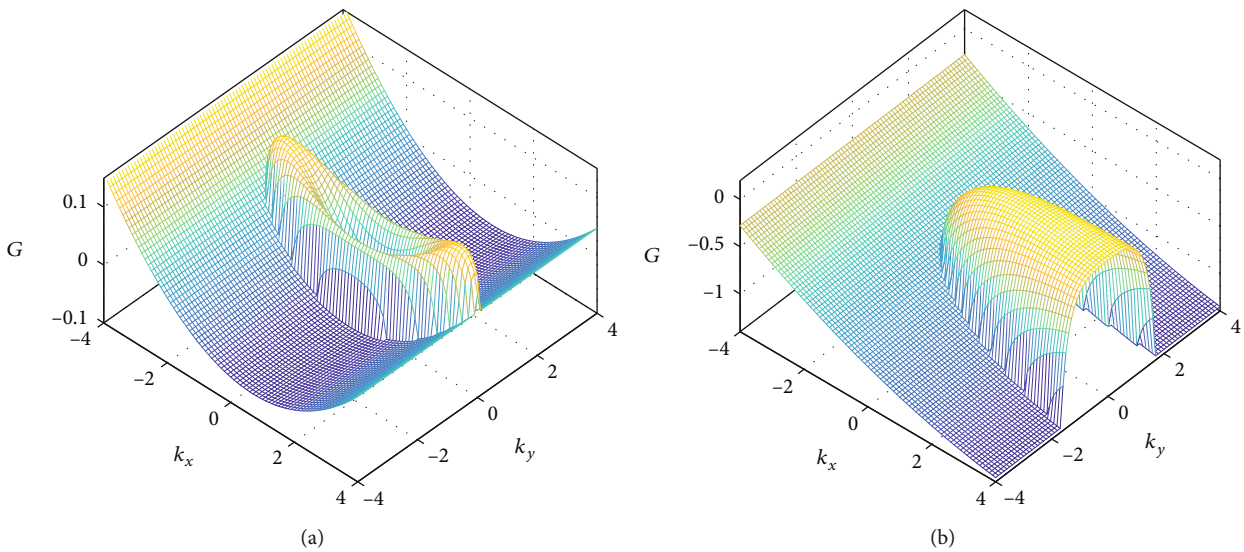

Figure 6: Growth rate instability obtained for $\alpha = 0.05$, $c_2 = 0.02$, $c_3 = 0.025$, $c_5 = 0.5$, and $\sigma = 0.02$. (a) $A_0 = 0.5$. (b) $A_0 = 1$.

The determinant of the matrix in Eq. (43) leads to the following characteristic equation:

$$\begin{aligned}\gamma^2 &+ \left(c_2 k_y \left(2k_0 - k_y\right) + \left(2\left(2A_0^2 c_5 - c_3\right)\right)A_0^2\right)\gamma \\ &+ \left(\frac{1}{4} c_2 k_y \left(2k_0 - k_y\right)^2 + \left(2k_0 - k_y\right)\left(2A_0^2 c_5 - c_3\right)A_0^2\right) c_2 k_y \\ &+ \frac{1}{4}\left(k_x^2 + \alpha k_y \left(k_y - 2k_0\right)\right)^2 - \left(1 - 2A_0^2\right) \\ &\cdot \left(kx^2 + \alpha k_y \left(k_y - 2k_0\right)\right)A_0^2 = 0,\end{aligned} \tag{44}$$

leading to the following solution:

$$\begin{aligned}\gamma &= -\left(c_2 k_y \left(k_0 - \frac{k_y}{2}\right) + \left(2A_0^2 c_5 - c_3\right)A_0^2\right) \pm \sqrt{-\delta}, \\ \delta &= \left(k_x^2 + \alpha k_y^2\right)\left(2A_0^4 - A_0^2 - \alpha k_y k_0 + \frac{1}{4}\left(k_x^2 + \alpha k_y^2\right)\right) \\ &\quad + \alpha k_0 k_y \left(\alpha k_y k_0 - 4A_0^4 + 2A_0^2\right) - A_0^4 \left(2A_0^2 c_5 - c_3\right)^2.\end{aligned} \tag{45}$$

The system is stable if $\delta > 0$, and for this case, one has $\lambda = -(c_2 k_y (k_0 - k_y/2) + (2A_0^2 c_5 - c_3)A_0^2) \pm i\omega$, with $\omega = \sqrt{\delta}$. Otherwise, it is possible to have the MI in the system governed by CQGLE (Eq. (1)) for some constraints on parameters k_x and k_y. The growth rate instability, defined by

$$G = \left(c_2 k_y \left(k_0 - k_y/2\right) + \left(2A_0^2 c_5 - c_3\right)A_0^2\right) + \sqrt{-\delta}, \tag{46}$$

and obtained for $\delta < 0$ quantifies the rapid for the appearing of MI. This rate is plotted in Figure 6 and justifies that the weak MI can also appear in the stability zone due to dissipation.

5. Conclusion and Perspective

In this paper, we have studied the 2D CQGLE given by Eq. (1) which can describe the dynamics of wave in some classes of physical systems by applying the bifurcation theory method of a planar dynamical system. This method is very powerful and efficient and is used to predict the type of solution of nonlinear partial differential (PDE) equations. Following this technique, the PDE is transformed to ODE from where the equilibrium points are found and phase portraits plotted. The phase portraits show separatrix which are curves separating classical solutions (bounded solutions) to nonclassical (unbounded) ones. Particularly, one has curves passing through three equilibrium points predicting the existence of a dark-dark soliton pair. One has in addition the curve starting from one fixed point, passing through another fixed point, and returning to the same fixed point predicting the existence of the pulse-dark soliton pair.

The analytical expression of the above-predicted solutions is found in the form of Jacobi elliptic functions for periodic solutions. The particular cases of these solutions leading to localized or nonperiodic solutions are also found. These solutions are plotted in 2D and 3D, respectively, justifying that the above solutions can predict some behaviours that can be found in some existing waveguides. These solutions can be so helpful for engineers, physicists, and mathematicians to justify some interesting phenomena observed in real-life problems.

It is important to mention that we have focused in this work on analytical results and the plotting of solutions. It should be interesting whether one can investigate solution degeneracy through the transmission between the orbits for different values of the included parameters, which would illustrate the validity of obtained solutions. The work in this light is now under consideration and will constitute a perspective for our future investigations.

Data Availability

The datasets generated during and/or analysed in the current study are available from the corresponding author on reasonable request.

Disclosure

The authors declare that they have carried out their work as part of their employment and as employers of the University of Douala (Cameroon) and the University of Ngaoundéré (Cameroon).

Conflicts of Interest

The authors declare that they have no conflict of interest.

Authors' Contributions

F. Waffo Tchuimmo, J. B. Gonpe Tafo, A. Chamgoue, N.C. Tsague Mezamo, F. Kenmogne, and L. Nana contributed equally to this work.

Acknowledgments

The authors would like to thank Research4Life for their financial support in publication. They are also grateful to the referees for their invaluable suggestions and comments for the improvement of the paper.

References

[1] M. C. Cross and P. C. Hohenberg, "Pattern formation outside of equilibrium," *Reviews of Modern Physics*, vol. 65, no. 3, pp. 851–1112, 1993.

[2] M. Golubitsky, I. N. Stewart, and D. G. Schaeffer, *Applied Mathematical Sciences Series*, Springer, Verlag, New York, 1988.

[3] M. Dennin, G. Ahlers, and D. S. Cannell, "Spatiotemporal chaos in electroconvection," *Science*, vol. 272, no. 5260, pp. 388–390, 1996.

[4] D. A. Egolf, I. V. Melnikov, W. Pesch, and R. E. Ecke, "Mechanisms of extensive spatiotemporal chaos in Rayleigh–Bénard convection," *Nature (London)*, vol. 404, no. 6779, pp. 733–736, 2000.

[5] A. M. Abouradia, T. S. El-Danaf, and A. M. Morad, "Exact solutions of the hierarchical Korteweg–de Vries equation of microstructured granular materials," *Chaos, Solitons & Fractals*, vol. 41, no. 2, pp. 716–726, 2009.

[6] A. M. Morad, S. M. A. Maize, A. A. Nowaya, and Y. S. Rammah, "A new derivation of exact solutions for incompressible magnetohydrodynamic plasma turbulence," *Journal of Nanofluids*, vol. 10, no. 98-105, 2021.

[7] A. M. Abourabia and A. M. Morad, "Exact traveling wave solutions of the van der Waals normal form for fluidized granular matter," *Physica A: Statistical Mechanics and its Applications*, vol. 16235, pp. 1–18, 2015.

[8] A. M. Morad, S. M. A. Maize, A. A. Nowaya, and Y. S. Rammah, "Stability analysis of magnetohydrodynamics waves in compressible turbulent plasma," *Journal of Nanofluids*, vol. 9, no. 3, pp. 196–202, 2020.

[9] A. M. Morad, E. S. Selima, and A. K. Abu-Nab, "Bubbles interactions in fluidized granular medium for the van der Waals hydrodynamic regime," *The European Physical Journal Plus*, vol. 136, no. 3, p. 306, 2021.

[10] W. van Saarloos, P. E. Cladis, and P. Palffy, *Reading*, Muhoray Addison Wesley, 1994.

[11] J. B. Gonpe Tafo, L. Nana, and T. C. Kofane, "Dynamics of a traveling hole in one-dimensional systems near subcritical bifurcation," *European Physical Journal Plus*, vol. 126, no. 11, p. 105, 2011.

[12] J. B. G. Tafo, L. Nana, and T. C. Kofane, "Nonlinear structures of traveling waves in the cubic–quintic complex Ginzburg–Landau equation on a finite domain," *Physica Scripta*, vol. 87, no. 6, article 065001, 2013.

[13] M. A. E. Abdelrahman and M. A. Sohaly, "On the new wave solutions to the MCH equation," *Indian Journal of Physics*, vol. 93, no. 7, pp. 903–911, 2019.

[14] X. F. Yang, Z. C. Deng, and Y. Wei, "A Riccati-Bernoulli sub-ODE method for nonlinear partial differential equations and its application," *Advances in Difference Equations*, vol. 2015, no. 1, 2015.

[15] K.-L. Geng, D.-S. Mou, and C.-Q. Dai, "Nondegenerate solitons of 2-coupled mixed derivative nonlinear Schrödinger equations," *Nonlinear Dynamics*, vol. 111, no. 1, pp. 603–617, 2023.

[16] W.-B. Bo, R.-R. Wang, Y. Fang, Y.-Y. Wang, and C.-Q. Dai, "Prediction and dynamical evolution of multipole soliton families in fractional Schrödinger equation with the PT-symmetric potential and saturable nonlinearity," *Nonlinear Dynamics*, vol. 111, no. 2, pp. 1577–1588, 2023.

[17] R.-R. Wang, Y.-Y. Wang, and C.-Q. Dai, "Influence of higher-order nonlinear effects on optical solitons of the complex Swift-Hohenberg model in the mode-locked fiber laser," *Optics and Laser Technology*, vol. 152, article 108103, 2022.

[18] J.-J. Fang, D.-S. Mou, H.-C. Zhang, and Y.-Y. Wang, "Discrete fractional soliton dynamics of the fractional Ablowitz-Ladik model," *Optik*, vol. 228, article 166186, 2021.

[19] X. Wen, R. Feng, J. Lin, W. Liu, F. Chen, and Q. Yang, "Distorted light bullet in a tapered graded-index waveguide with PT symmetric potentials," *Optik*, vol. 248, article 168092, 2021.

[20] H.-Y. Wu and L.-H. Jiang, "One-component and two-component Peregrine bump and integrated breather solutions for a partially nonlocal nonlinearity with a parabolic potential," *Optik*, vol. 262, article 169250, 2022.

[21] Y. Fang, G.-Z. Wu, Y.-Y. Wang, and C.-Q. Dai, "Data-driven femtosecond optical soliton excitations and parameters discovery of the high-order NLSE using the PINN," *Nonlinear Dynamics*, vol. 105, no. 1, pp. 603–616, 2021.

[22] C. Q. Dai and J. F. Zhang, "Jacobian elliptic function method for nonlinear differential-difference equations," *Chaos, Solitons and Fractals*, vol. 27, no. 4, pp. 1042–1047, 2006.

[23] P. Zhong, R. Yang, and G. Yang, "Exact periodic and blow up solutions for 2D Ginzburg–Landau equation," *Physics Letters A*, vol. 373, no. 1, pp. 19–22, 2008.

[24] A. E. L. Achab, H. Rezazadeh, D. Baleanu, T. D. Leta, S. Javeed, and K. S. Alimgeer, "Ginzburg Landau equation's Innovative Solution (GLEIS)," *Physica Scripta*, vol. 96, no. 3, article 035204, 2021.

[25] H. Bulut, T. A. Sulaiman, and H. M. Baskonus, "On the new soliton and optical wave structures to some nonlinear evolution equations," *European Physical Journal Plus*, vol. 132, no. 11, p. 459, 2017.

[26] M. Eslami, "Trial solution technique to chiral nonlinear Schrodinger's equation in (1+ 2)-dimensions," *Nonlinear Dynamics*, vol. 85, no. 2, pp. 813–816, 2016.

[27] A. M. Abourabia, K. M. Hassan, and A. M. Morad, "Analytical solutions of the magma equations for molten rocks in a granular matrix," *Chaos, Solitons & Fractals*, vol. 42, no. 2, pp. 1170–1180, 2009.

[28] A. A. Elmandouh, "Bifurcation and new traveling wave solutions for the 2D Ginzburg–Landau equation," *The European Physical Journal Plus*, vol. 135, no. 8, p. 648, 2020.

[29] H. Sakaguchi and B. A. Malomed, "Stable localized pulses and zigzag stripes in a two-dimensional diffractive–diffusive Ginzburg–Landau equation," *Physica D*, vol. 159, no. 1-2, pp. 91–100, 2001.

[30] Y.-q. Shi, Z.-d. Dai, and S. Han, "Exact solutions for 2D cubic-quintic Ginzburg-Landau equation," *Journal of Physics: Conference Series*, vol. 96, article 12148, 2008.

[31] O. V. Shtyrina, I. A. Yarutkina, A. S. Skidin, E. V. Podivilov, and M. P. Fedoruk, "Theoretical analysis of solutions of cubic-quintic Ginzburg-Landau equation with gain saturation," *Optics Express*, vol. 27, no. 5, p. 5, 2019.

[32] A. El Achab and A. Amine, "A construction of new exact periodic wave and solitary wave solutions for the 2D Ginzburg–Landau equation," *Nonlinear Dynamics*, vol. 91, no. 2, pp. 995–999, 2018.

[33] A. R. Seadawy, M. Arshad, and D. Lu, "The weakly nonlinear wave propagation theory for the Kelvin-Helmholtz instability in magnetohydrodynamics flows," *Chaos, Solitons and Fractals*, vol. 139, article 110141, 2020.

[34] K. Shehzad, A. R. Seadawy, J. Wang, and M. Arshad, "Multi peak solitons and btreather types wave solutions of unstable NLSEs with stability and applications in optics," *Optical and Quantum Electronics*, vol. 55, no. 1, 2022.

[35] I. S. Aranson and L. Kramer, "The world of the complex Ginzburg-Landau equation," *Reviews of Modern Physics*, vol. 74, no. 1, pp. 99–143, 2002.

[36] A. Belandez, T. Belandez, F. J. Martinez, C. Pascual, M. L. Alvarez, and E. Arribas, "Exact solution for the unforced Duffing oscillator with cubic and quintic nonlinearities," *Nonlinear Dynamics*, vol. 86, no. 3, pp. 1687–1700, 2016.

[37] P. F. Byrd and M. D. Fridman, *Handbook of Elliptic Integrals for Engineers and Scientists*, Springer, Berlin, 1971.

[38] N. Bekki and K. Nozaki, "Formations of spatial patterns and holes in the generalized Ginzburg-Landau equation," *Physics Letters A*, vol. 110, no. 3, pp. 133–135, 1985.

[39] I. S. Gradshteyn and I. M. Ryzhik, *Table of Integrals, Series and Products*, Academic Press, San Diego, Sixth edition, 2000.

[40] F. Kenmogne and D. Yemélé, "Bright and peaklike pulse solitary waves and analogy with modulational instability in an extended nonlinear Schrödinger equation," *Physical Review E*, vol. 88, no. 4, article 043204, 2013.

[41] M. Arshad, D. Lu, M.-U. Rehman, I. Ahmed, and A. M. Sultan, "Optical solitary wave and elliptic function solutions of the Fokas–Lenells equation in the presence of perturbation terms and its modulation instability," *Physica Scripta*, vol. 94, no. 10, article 105202, 2019.

[42] J. B. T. Gonpe, F. Kenmogne, A. K. Mando, R. Eno, and D. Yemélé, "Modulated solitons and transverse stability in a two-dimensional nonlinear reaction diffusion electrical network," *Results in Physics*, vol. 50, article 106532, 2023.

[43] I. S. M. Rayhanul, *Stability analysis and soliton solutions to the new Hamiltonian amplitude equation in mathematical physics*, Research square, 2022.

[44] F. Kenmogne and D. Yemélé, "Exotic modulated signals in a nonlinear electrical transmission line: modulated peak solitary wave and gray compacton," *Chaos, Solitons and Fractals*, vol. 45, no. 1, pp. 21–34, 2012.